Electronic Supplementary Material (ESI) for Green Chemistry.

Supporting Information

Designable synthesis of reactive deep eutectic solvents (RDESs) in regulating Ni-based materials for efficient oxygen evolution reaction

Yahui Wei,[a]‡ Jingyun Jiang,[a]‡ Jialong Dong,[a] Yifan Xu,[a] Jianwei Fu, *[a] and Qun Xu*[ab]

[a]College of Materials Science and Engineering, Zhengzhou University, Zhengzhou 450001, P. R. China.

[b]Henan Institute of Advanced Technology, Zhengzhou University, Zhengzhou 450001, P. R. China.

E-mail: jwfu@zzu.edu.cn; qunxu@zzu.edu.cn

‡The authors contributed equally to this work.

Tables of contents

1. Supplementary Figures and Tables

Table S8 Assignments of the FTIR of Arg-$NiCl_2 \cdot 6H_2O$ and the related arginine.

Table S9 The reactive decomposition temperatures ($T_{reactive}$) and onset temperatures (T_{onset}) of the synthesized RDESs.

Table S10 The OER performance of 2D Ni/$Ni(OH)_2$ in similar alkaline media and other representative reported non-precious metal electrocatalysts.

2. Reference

1. Supplementary Figures and Tables

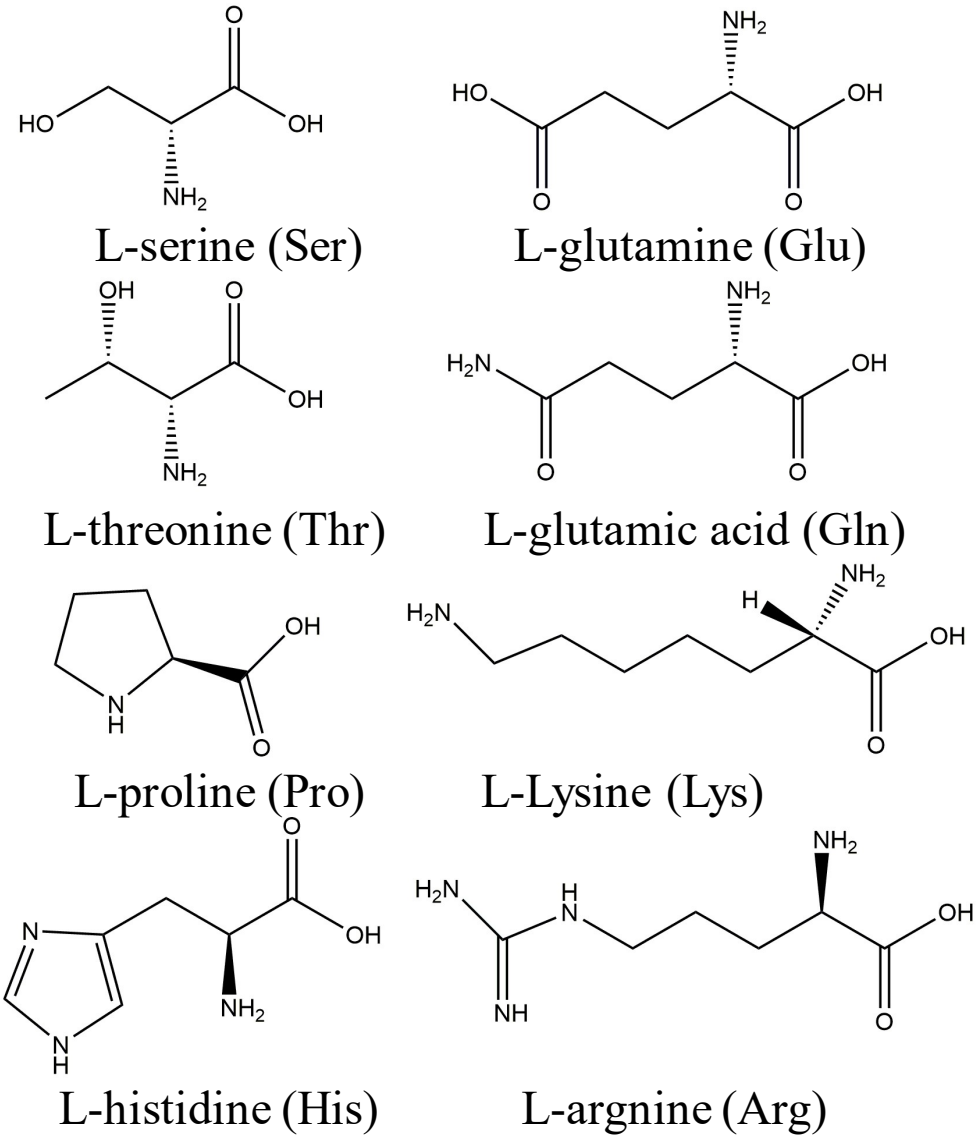

Figure S1 Structure of the selected eight amine acids.

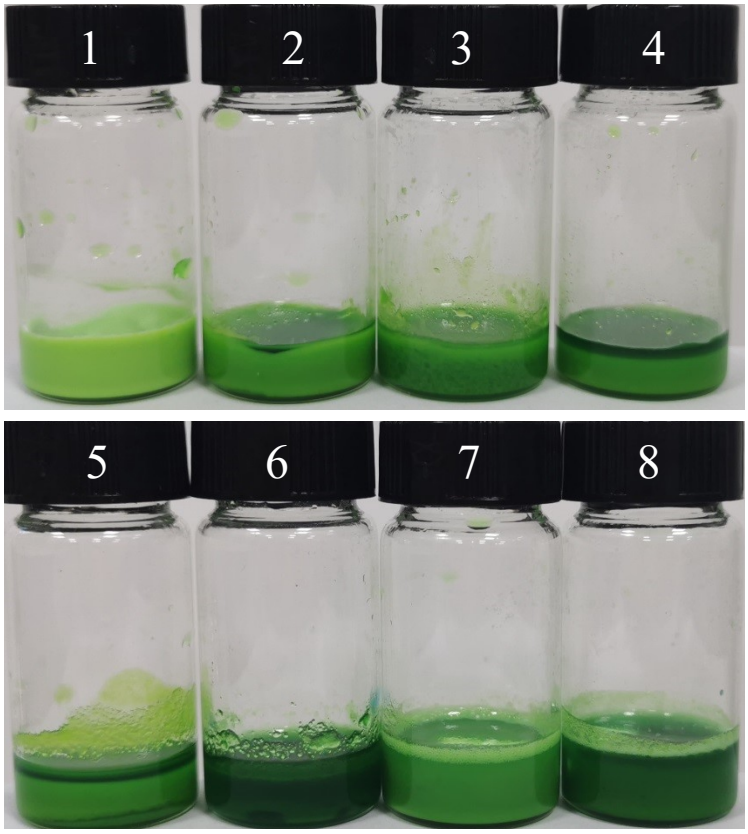

Figure S2 Photograph of the synthesized RDESs: 1 Ser-$NiCl_2 \cdot 6H_2O$, 2 Thr-$NiCl_2 \cdot 6H_2O$, 3 Glu-$NiCl_2 \cdot 6H_2O$, 4 Gln-$NiCl_2 \cdot 6H_2O$, 5 Pro-$NiCl_2 \cdot 6H_2O$, 6 His-$NiCl_2 \cdot 6H_2O$,7 Lys-$NiCl_2 \cdot 6H_2O$, 8 Arg-$NiCl_2 \cdot 6H_2O$.

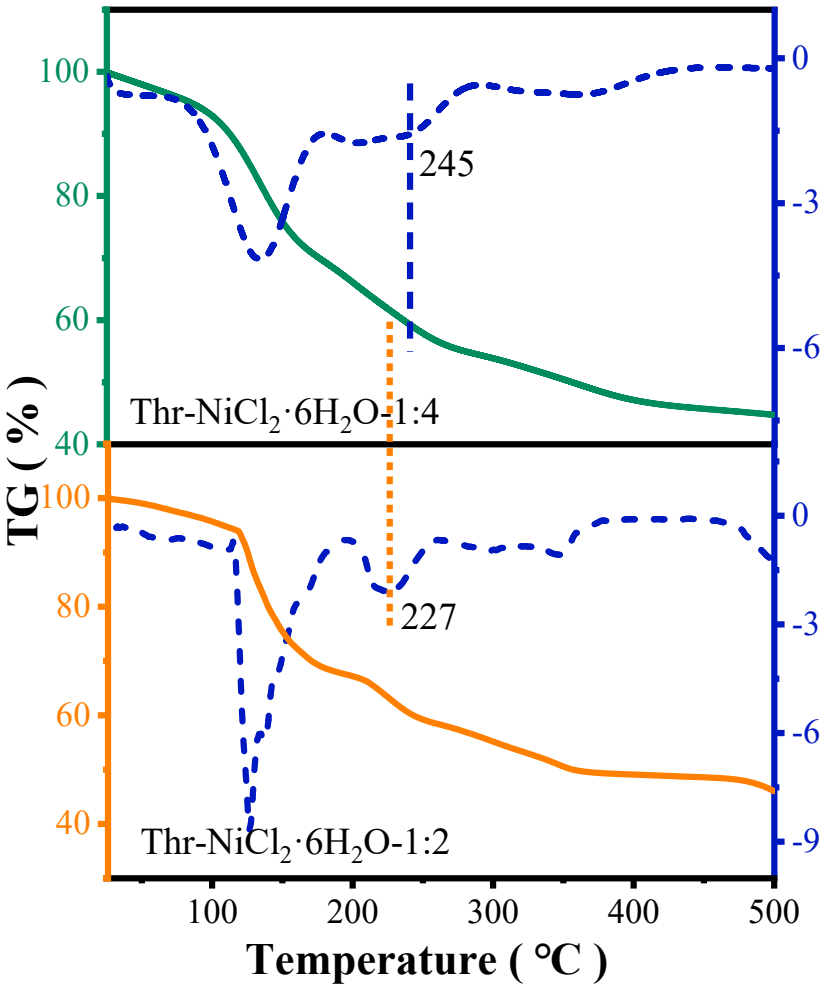

Figure S3 TGA curves of the Thr-$NiCl_2$·6H2O at the molar ratio of 1:4 (above) and 1:2 (below).

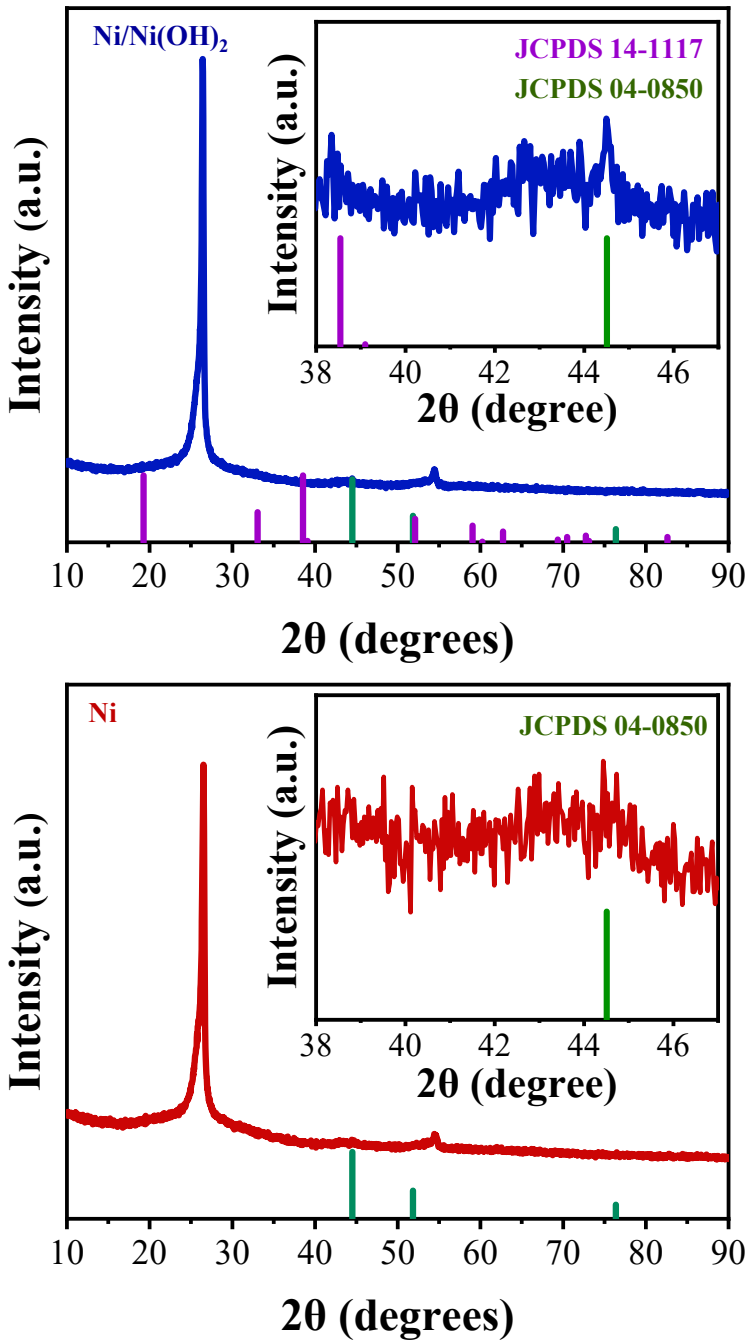

Figure S4 XRD pattern of $Ni/Ni(OH)_2$ nanosheets (a) and Ni nanoparticles (b) grown on the CPs.

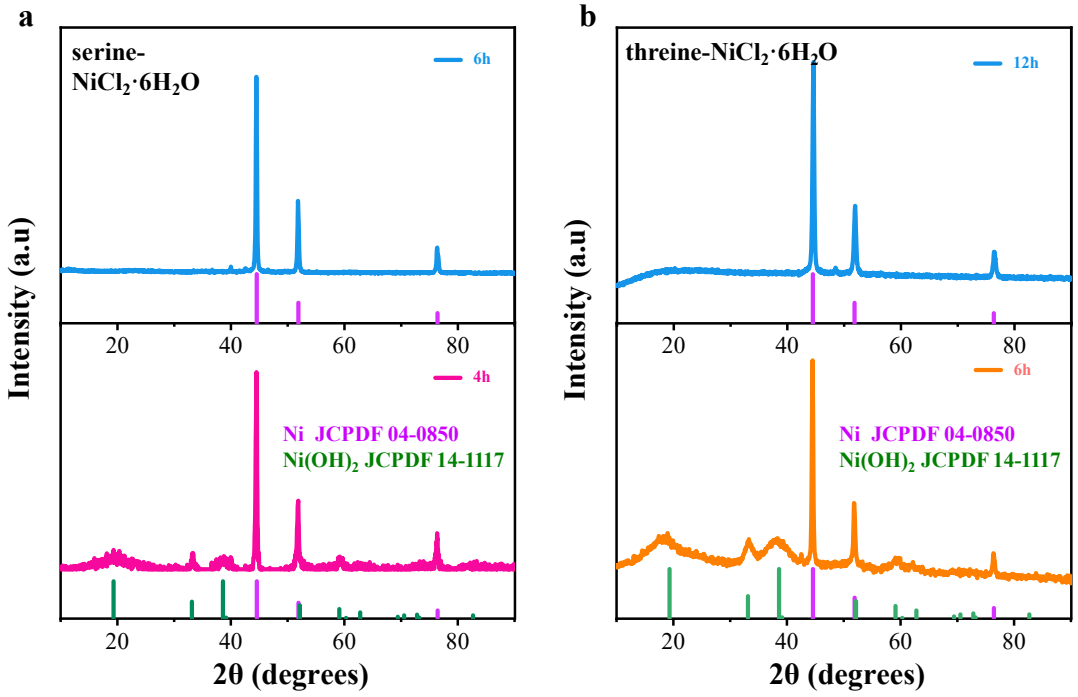

Figure S5 XRD pattern of the samples derived from serine-$NiCl_2 \cdot 6H_2O$ system (a) and threonine-$NiCl_2 \cdot 6H_2O$ (b) at different times.

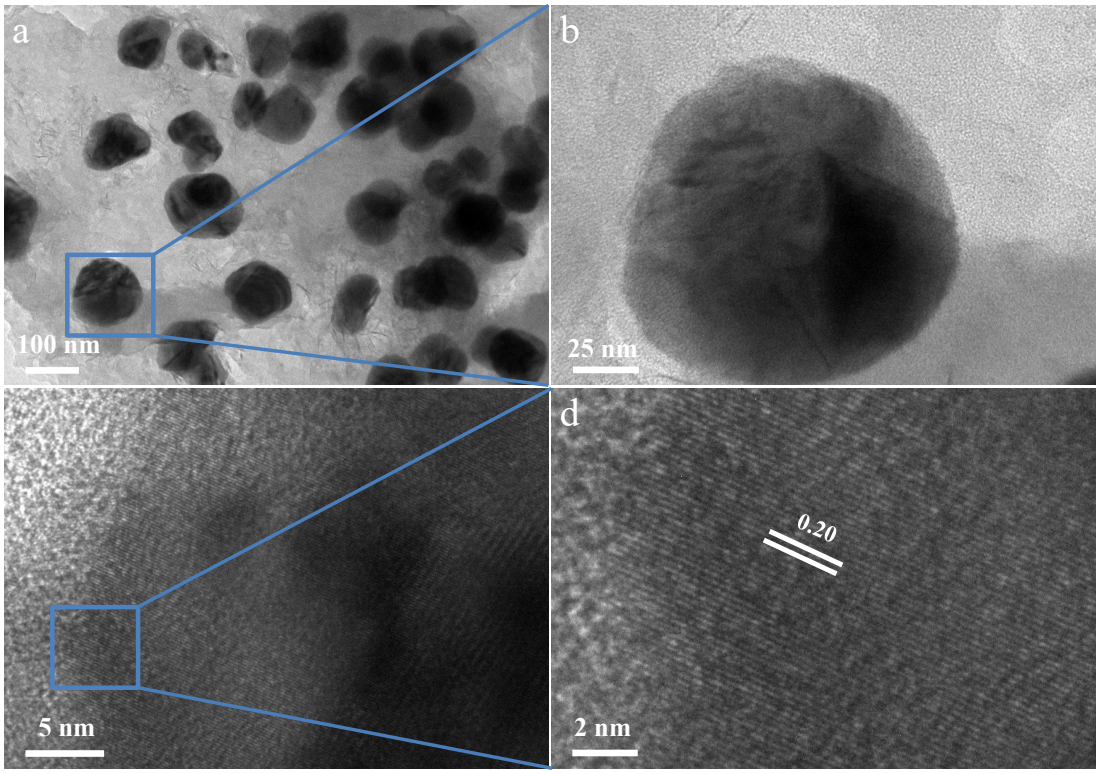

Figure S6 (a) TEM and (b) HRTEM images of the obtained Ni nanoparticles.

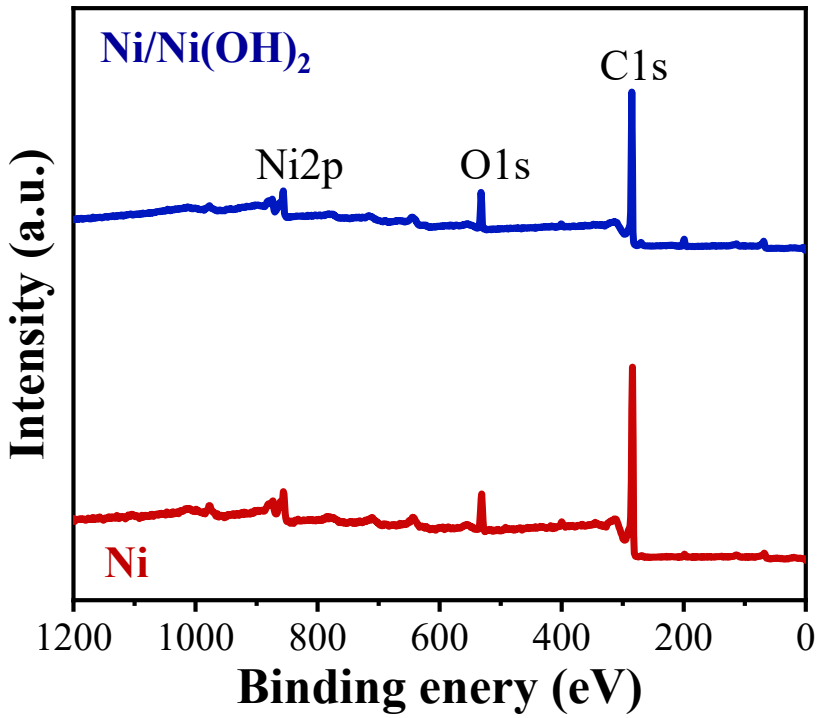

Figure S7 The XPS survey spectrum of the Ni (below) and Ni/Ni(OH)$_2$ (above) samples.

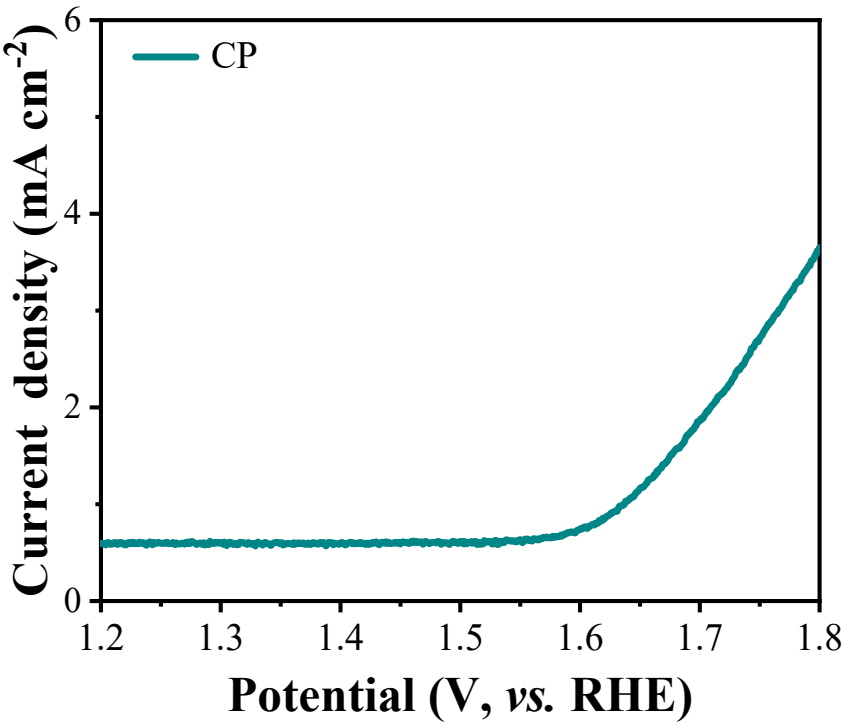

Figure S8 LSV curves for bare carbon papers with 90% iR correction at a sweep rate of 5 mV s^{-1}.

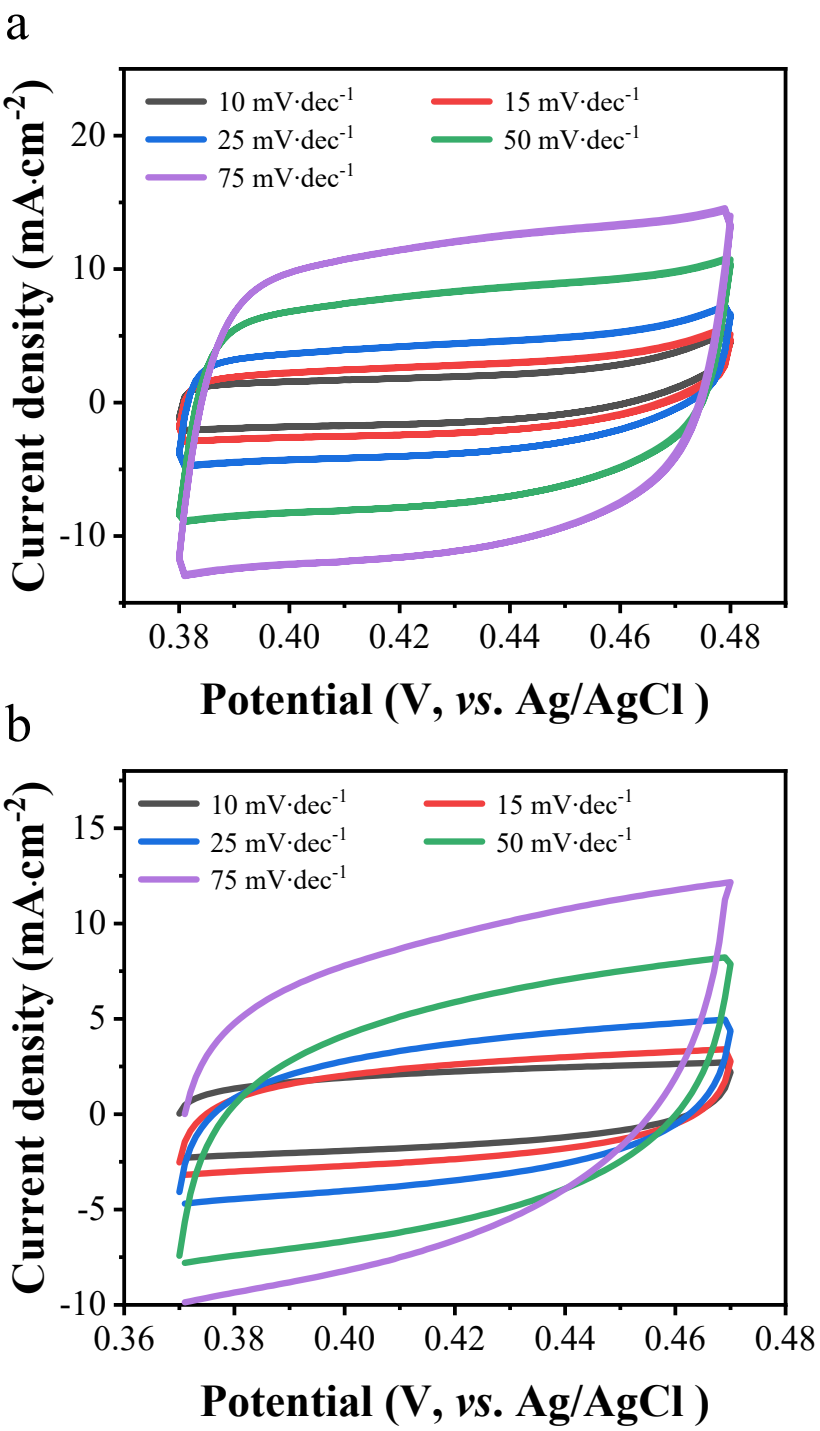

Figure S9 Cyclic voltammograms of (a) Ni/Ni(OH)$_2$ and (b) Ni nanoparticles at scan rates from 10 to 75 mV s^{-1}.

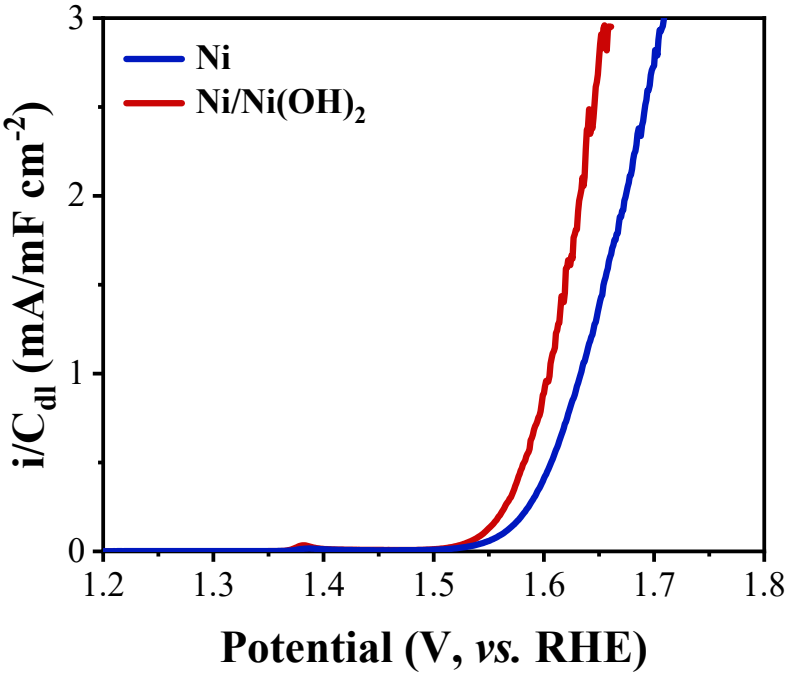

Figure S10 LSV curves of 2D $Ni/Ni(OH)_2$ (red) and Ni nanoparticles (blue) after normalized with C_{dl}.

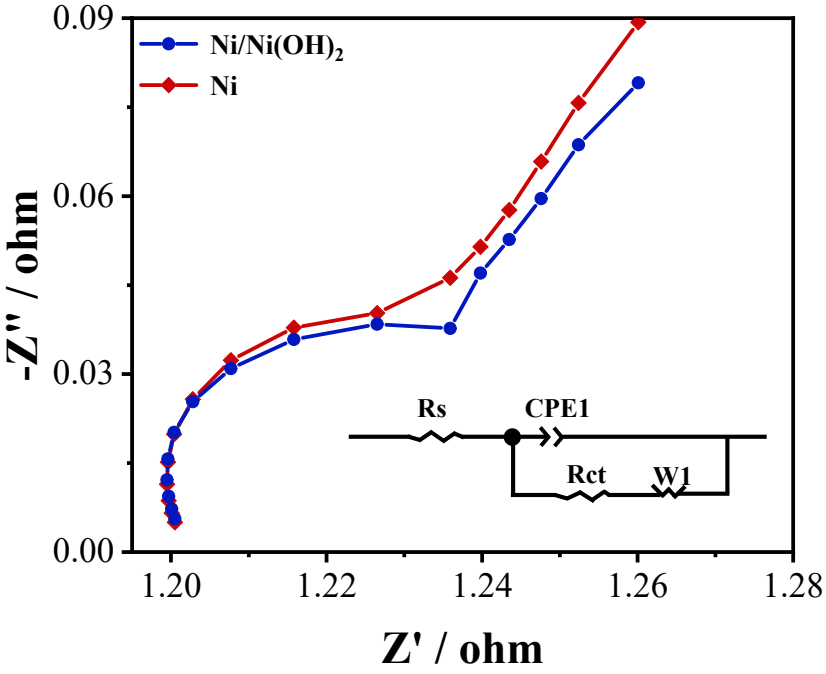

Figure S11 Nyquist plots and the related fitting curves of Ni (red) and $Ni/Ni(OH)_2$ (blue).

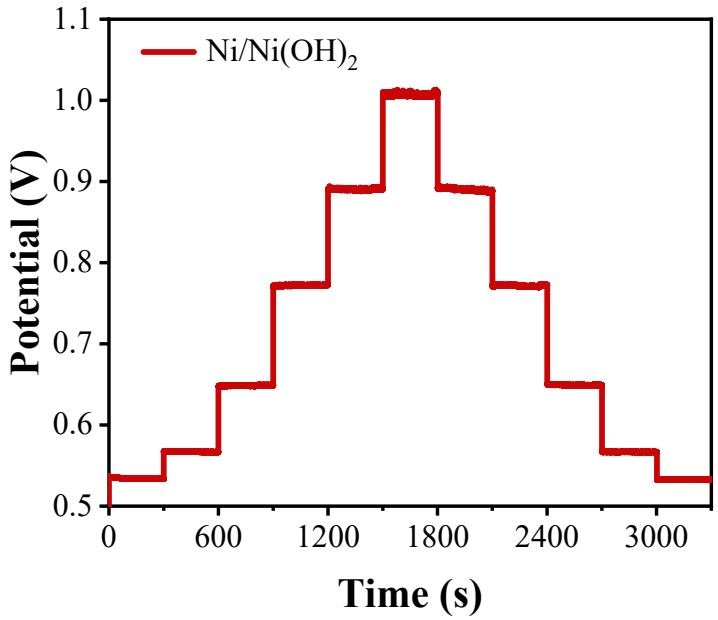

Figure S12 Multi-current step curves of 2D Ni/Ni(OH)$_2$.

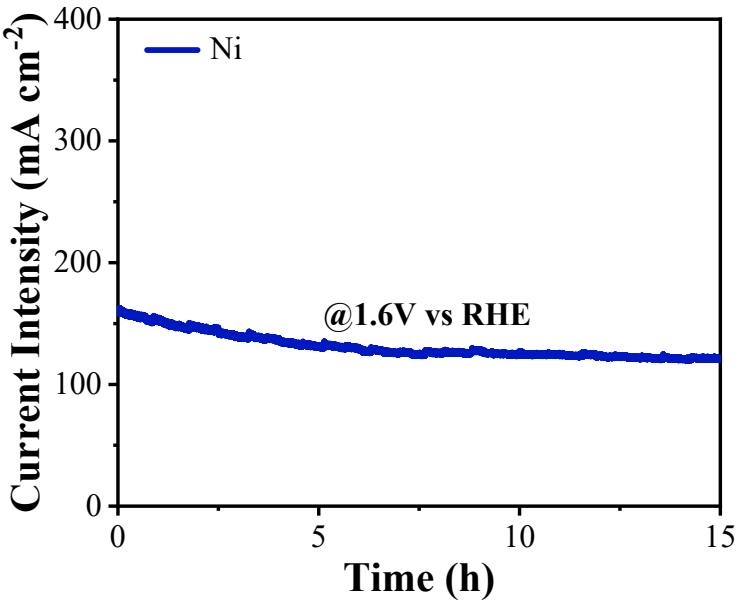

Figure S13 Chronoamperometric curve of Ni nanoparticles at 1.6 V (vs RHE) for 15 h.

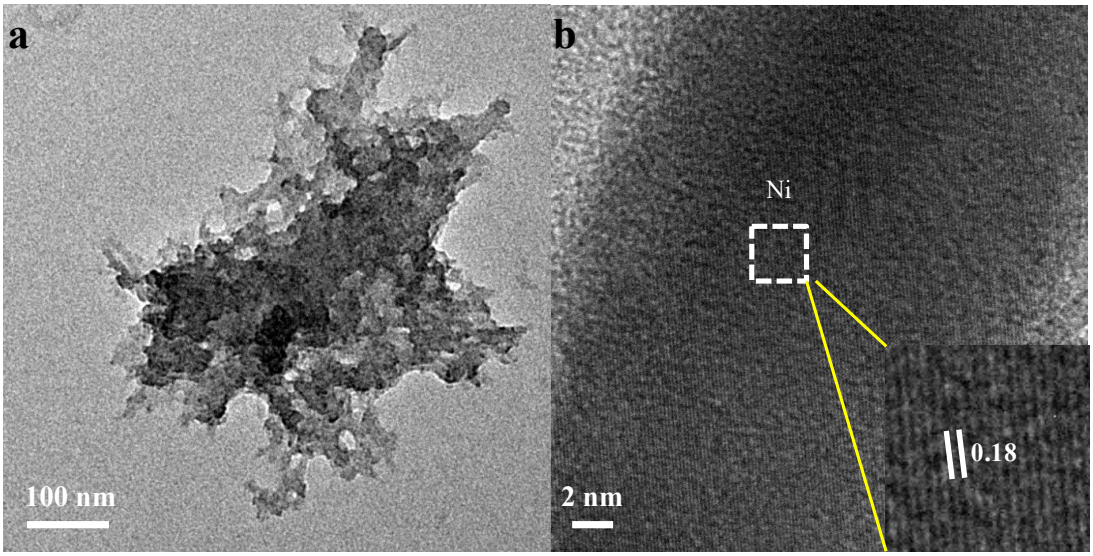

Figure S14 TEM(a) and HRTEM(b) images of Ni/Ni(OH)$_2$ nanosheets after long-term OER test.

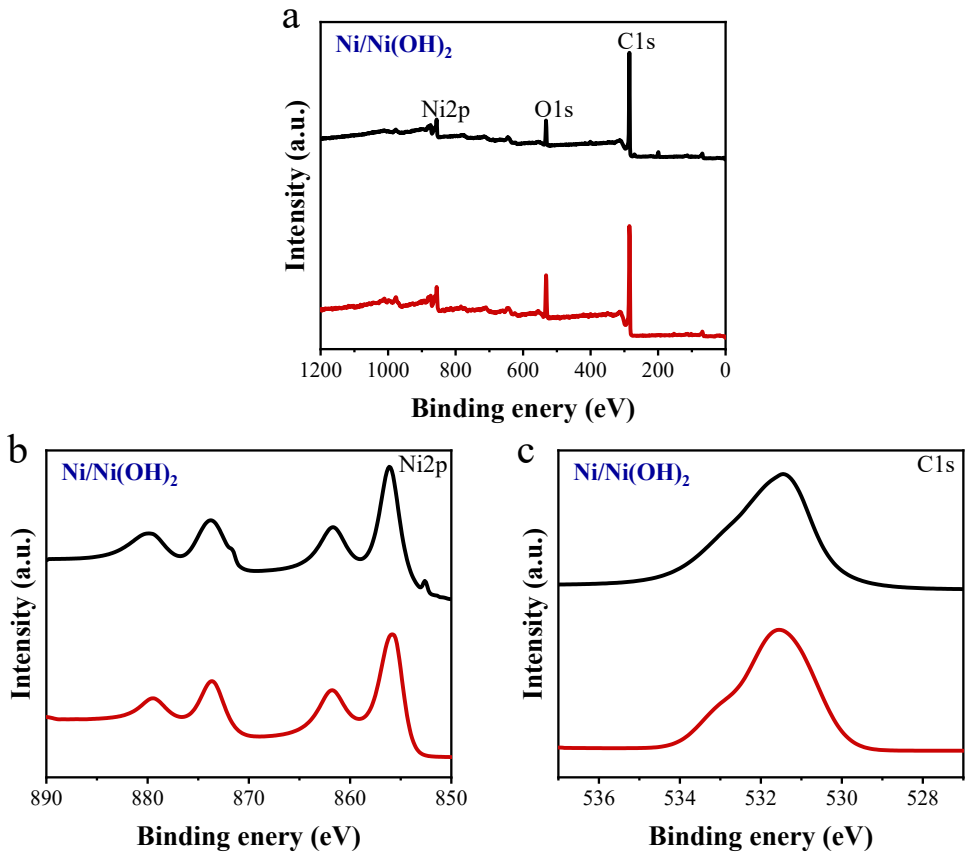

Figure S15 XPS spectra of the 2D Ni/Ni(OH)$_2$ samples initial (above) and a long-term OER test (below) : (a) the full spectra, (b) Ni 2p and (c) O 1s.

Table S1 Assignments of the FTIR of Ser-$NiCl_2 \cdot 6H_2O$ and the related serine.[1]

Groups	Vibration	Absorption band of serine, cm^{-1}	Absorption band of Ser-$NiCl_2 \cdot 6H_2O$, cm^{-1}
NH_3^+	τ	531	500-700 with max at 650
COO^-	δ	613	
C-N	ν	1014	1045
COO^-	ν_{symm}	1411	1434
	ν_{as}	1600	1628
NH_3^+	ν_{symm}	2040	no
NH_3^+	ν	2500-3350	2500-3500 with max at 3344
O-H	ν	3465	

ν, bond stretching; δ, in-plane bending; γ, out-of-plane bending; ω, wagging; τ, twisting; as, asymmetric; s, symmetric

Table S2 Assignments of the FTIR of Thr-$NiCl_2 \cdot 6H_2O$ and the related threonine.[2]

Groups	Vibration	Absorption band of threonine, cm^{-1}	Absorption band of Thr-$NiCl_2 \cdot 6H_2O$, cm^{-1}
NH_3^+	τ	531	
COO^-	γ	563	500-700 with max at 659
	ω	701	
C-N	ν	1041	1041
NH_3^+	γ	1112	1077
COO^-	ν_{symm}	1417	1435
COO^-	ν_{as}	1628	1628
NH_3^+	ν_{symm}	2050	no
N-H, O-H,C-H	ν	2100-3400 with max at 2975	2500-3700 with max at 3344

ν, bond stretching; δ, in-plane bending; γ, out-of-plane bending; ω, wagging; τ, twisting; as, asymmetric; s, symmetric

Table S3 Assignments of the FTIR of Glu-$NiCl_2 \cdot 6H_2O$ and the related glutamic acid[3, 4]

Groups	Vibration	Absorption band of glutamic acid, cm^{-1}	Absorption band of Glu-$NiCl_2 \cdot 6H_2O$, cm^{-1}
C=O	γ	540	500-700 with max at 676
NH_3^+	ν_{symm}	1505	1505
COO^-	ν_{symm}	1668	1700
NH_3^+	ν_{symm}	2081	no
N-H, C-H	ν	2800-3300 with max at 3056	2500-3700 with max at 3320

ν, bond stretching; δ, in-plane bending; γ, out-of-plane bending; ω, wagging; τ, twisting; as, asymmetric; s, symmetric

Table S4 Assignments of the FTIR of Gln-$NiCl_2 \cdot 6H_2O$ and the related glutamine.[5]

Groups	Vibration	Absorption band of glutamine, cm^{-1}	Absorption band of Gin-$NiCl_2 \cdot 6H_2O$, cm^{-1}
	γ	540	
C=O	δ	622	500-700 with max at 620
	ω	654	
NH_3^+	γ	1131	1147
	δ	1489	1500
COO^-	ν	1635	1654
NH_3^+	ν_{symm}	2041	no
C-H	ν	2932	
CH_2	ν	3173	2500-3700 with max at 3340
NH_3^+	ν_{as}	3408	
	ν_{symm}	3215	

ν, bond stretching; δ, in-plane bending; γ, out-of-plane bending; ω, wagging; τ, twisting; as, asymmetric; s, symmetric

Table S5 Assignments of the FTIR of Pro-$NiCl_2 \cdot 6H_2O$ and the related proline.[6]

Groups	Vibration	Absorption band of proline, cm^{-1}	Absorption band of Pro-$NiCl_2 \cdot 6H_2O$, cm^{-1}
CH_2	ρ	800,852	500-800 with max at 670
ring	δ	642	
CH	δ	1294	1328
O-H	δ	1377	1423
N-H	δ	1548	1560
COO^-	ν	1630	1630
CH_2	ν_s	2938,2956	2700-3700 with max at 3300
	ν_{as}	3012,2978	
N-H	ν	3410	
O-H	ν	3518	

ν, bond stretching; δ, in-plane bending; γ, out-of-plane bending; ω, wagging; τ, twisting; as, asymmetric; s, symmetric

Table S6 Assignments of the FTIR of His-$NiCl_2 \cdot 6H_2O$ and the related histidine.[7]

Groups	Vibration	Absorption band of histidine, cm^{-1}	Absorption band of His-$NiCl_2 \cdot 6H_2O$, cm^{-1}
C-H of ring	δ	540	
C-H	δ	624,686	500-800 with max at 630
N-H	γ	925,964	
N-H	δ	1568	1583
COO^-	ν	1640	1640
NH_3^+	ν_{symm}	2019	no
CH_2	ν	2615,2992	2700-3700 with max at 3300
C-H of ring	ν	3109	

ν, bond stretching; δ, in-plane bending; γ, out-of-plane bending; ω, wagging; τ, twisting; as, asymmetric; s, symmetric

Table S7 Assignments of the FTIR of Lys-$NiCl_2 \cdot 6H_2O$ and the related lysine.[8]

Groups	Vibration	Absorption band of lysine, cm^{-1}	Absorption band of Lys-$NiCl_2 \cdot 6H_2O$, cm^{-1}
O-H	δ	497	
COO^-	ν	551	500-800 with max at 657
	ν	729	
COO^-	ν_{symm}	1414	1414
NH_3^+	ν_{as}	1515	1515
COO^-	ν_{symm}	1589	1612
CH_2	ν	2937	2700-3700 with max at 3300
NH_3^+	ν	3361	

ν, bond stretching; δ, in-plane bending; γ, out-of-plane bending; ω, wagging; τ, twisting; as, asymmetric; s, symmetric

Table S8 Assignments of the FTIR of Arg-$NiCl_2 \cdot 6H_2O$ and the related arginine.[9]

Groups	Vibration	Absorption band of arginine, cm^{-1}	Absorption band of Arg-$NiCl_2 \cdot 6H_2O$, cm^{-1}
CNH	ν	794	
O-H	δ	1334	1353
NH_3^+	ν_{as}	1550	1573
COO^-	ν_{as}	1620	1666
NH_3^+	γ	1680	
CH_2	ν_{symm}	2928	2700-3700 with max at 3300
NH_3^+	ν	3151	

ν, bond stretching; δ, in-plane bending; γ, out-of-plane bending; ω, wagging; τ, twisting; as, asymmetric; s, symmetric

Table S9 The reactive decomposition temperatures ($T_{reactive}$) and onset temperatures (T_{onset}) of the synthesized RDESs.

RDESs	$T_{reactive}$ (^oC)	T_{onset} (^oC)
Thr-$NiCl_2 \cdot 6H_2O$	227.5	126.5
Ser-$NiCl_2 \cdot 6H_2O$	224.4	124.7
Gln-$NiCl_2 \cdot 6H_2O$	216	123.8
Glu-$NiCl_2 \cdot 6H_2O$	215	122.8
His-$NiCl_2 \cdot 6H_2O$	293	121.9
Pro-$NiCl_2 \cdot 6H_2O$	284	125.5
Arg-$NiCl_2 \cdot 6H_2O$	310	122
Lys-$NiCl_2 \cdot 6H_2O$	334.8	122

Table S10 The OER performance of 2D Ni/Ni(OH)$_2$ in similar alkaline media and other representative reported non-precious metal electrocatalysts.

Electrocatalysts	Current density (mA cm^{-2})	Overpotential (mV)	Tafel slopes (mV dec^{-1})	References
2D Ni/Ni(OH)$_2$	**100**	**326**	**51**	**This work**
	1000	**395**		
Ni	**100**	**358**	**62**	**This work**
	1000	**457**		
Ni/Ni(OH)$_2$	10	270	70	10
Co_3O_4–Mo_2N NFs	41.9	300	87.8	11
Ni-BDC/Ni(OH)$_2$	10	320	41	12
Ni/Ni(OH)$_2$	10	310	74.8	13
NiFe-LDH@NiCu	20	300	56.9	14
NrN@Ni	10	313	46	15
d-NiFe-LDH	10	230	77	16
	50	290		
NM50-Ni_3S_4	10	307	67	17
Ni-N-O	10	300	74	18
Co(s)-Fe(s)	10	355	62	19
$Ni(CN)_2$/$NiSe_2$	100	470	68	20
Fe-NiO/NiS_2	10	270	40	21
$NiS_{1.03}$-NSC	10	270	68.9	22
$NiCo_2S_4$	10	337	64	23
2D $[Co(NH_3)_4CO_3]Cl$	10	291	64	24
OV-Fe-DES	100	298	49	25
$NiFe_{0.05}$-N-CP	100	320	76	26

2. Reference

1. S. Jarmelo, I. Reva, P. Carey and R. Fausto, *Vib. Spectrosc.*, 2007, **43**, 395-404.
2. G. R. Kumar, S. G. Raj, R. Mohan and R. Jayavel, *J. Cryst. Growth*, 2005, **275**, e1947-e1951.
3. E. Greiner, K. Kumar, M. Sumit, A. Giuffre, W. Zhao, J. Pedersen and N. Sahai, *Geochim. Cosmochim. Acta*, 2014, **133**, 142-155.
4. J. Schöll, L. Vicum, M. Müller and M. Mazzotti, *Chem. Eng. Technol.*, 2006, **29**, 257-264.
5. A. Pawlukojć, K. Hołderna-Natkaniec, G. Bator and I. Natkaniec, *Chem. Phys*, 2014, **443**, 17-25.
6. Y. S. Mary, L. Ushakumari, B. Harikumar, H. T. Varghese and C. Y. Panicker, *J. Iran. Chem. Soc.*, 2009, **6**, 138-144.
7. A. Petrosyan, *Vib. Spectrosc.*, 2007, **43**, 284-289.
8. M. B. Mary, M. Umadevi and V. Ramakrishnan, *Spectrochim. Acta, Part A*, 2005, **61**, 3124-3130.
9. S. Kumar and S. Rai, 2010.
10. L. Dai, Z. N. Chen, L. Li, P. Yin, Z. Liu and H. Zhang, *Adv. Mater.*, 2020, **32**, 1906915.
11. T. Wang, P. Wang, W. Zang, X. Li, D. Chen, Z. Kou, S. Mu and J. Wang, *Adv. Funct. Mater.*, 2022, **32**, 2107382.
12. D. Zhu, J. Liu, L. Wang, Y. Du, Y. Zheng, K. Davey and S.-Z. Qiao, *Nanoscale*, 2019, **11**, 3599-3605.
13. D. Lim, S. Kim, N. Kim, E. Oh, S. E. Shim and S.-H. Baeck, *ACS Sustainable Chem. Eng*, 2020, **8**, 4431-4439.
14. Y. Zhou, Z. Wang, Z. Pan, L. Liu, J. Xi, X. Luo and Y. Shen, *Adv. Mater.*, 2019, **31**, 1806769.
15. D. Shao, P. Li, D. Wang, C. Zhao and C. Zhao, *J. Solid State Electrochem.*, 2019, **23**, 2051-2060.
16. Y. j. Wu, J. Yang, T. x. Tu, W. q. Li, P. f. Zhang, Y. Zhou, J. f. Li, J. t. Li and S. G. Sun, *Angew. Chem., Int. Ed.*, 2021, **60**, 26829-26836.
17. K. Wan, J. Luo, C. Zhou, T. Zhang, J. Arbiol, X. Lu, B. W. Mao, X. Zhang and J. Fransaer, *Adv. Funct. Mater.*, 2019, **29**, 1900315.
18. J. Huang, Y. Sun, X. Du, Y. Zhang, C. Wu, C. Yan, Y. Yan, G. Zou, W. Wu and R. Lu, *Adv. Mater.*, 2018, **30**, 1803367.
19. C. Maccato, L. Bigiani, L. Girardi, A. Gasparotto, O. I. Lebedev, E. Modin, D. Barreca and G. A. Rizzi, *Adv. Mater. Interfaces*, 2021, **8**, 2100763.
20. J. Nai, X. Xu, Q. Xie, G. Lu, Y. Wang, D. Luan, X. Tao and X. W. Lou, *Adv. Mater.*, 2022, **34**, 2104405.
21. N. Zhang, Y. Hu, L. An, Q. Li, J. Yin, J. Li, R. Yang, M. Lu, S. Zhang, P. Xi and C.-H. Yan, *Angew. Chem., Int. Ed.*, 2022, **134**, 202207217.
22. H. Yang, C. Wang, Y. Zhang and Q. Wang, *Small*, 2018, **14**, 1703273.
23. J. Jiang, C. Yan, X. Zhao, H. Luo, Z. Xue and T. Mu, *Green Chem.*, 2017, **19**, 3023-3031.
24. S. Liu, C. Zhang, B. Zhang, Z. Li and J. Hao, *ACS Sustainable Chem. Eng*, 2019, **7**, 8964-8971.
25. S. Liu, T. Chen, H. Ying, Z. Li and J. Hao, *Adv. Sustainable Syst.*, 2020, **4**, 2000038.
26. Y. Xu, Z. Cheng, J. Jiang, J. Du and Q. Xu, *Chem. Commun.*, 2021, **57**, 13170-13173.